Published in final edited form as:
Biomaterials. 2012 November ; 33(33): 8353–8362. doi:10.1016/j.biomaterials.2012.08.018.

The effect of glycomimetic functionalized collagen on peripheral nerve repair

Shirley N. Masand[a], **Jian Chen**[b], **Isaac J. Perron**[a], **Babette C. Hammerling**[c], **Gabriele Loers**[d], **Melitta Schachner**[b,e,**], and **David I. Shreiber**[a,*]

[a]Department of Biomedical Engineering, Rutgers, The State University of New Jersey, 599 Taylor Road, Piscataway, NJ 08854, USA

[b]W.M. Keck Center for Collaborative Neuroscience, Rutgers, The State University of New Jersey, USA

[c]School of Environmental and Biological Sciences, Rutgers, The State University of New Jersey, USA

[d]Center for Molecular Neurobiology, University Hospital Hamburg-Eppendorf, Hamburg, Germany

[e]Center for Neuroscience, Shantou University Medical College, 22 Xin Ling Road, Shantou 515041, China

Abstract

Increasing evidence suggests that the improper synaptic reconnection of regenerating axons is a significant cause of incomplete functional recovery following peripheral nerve injury. In this study, we evaluate the use of collagen hydrogels functionalized with two peptide glycomimetics of naturally occurring carbohydrates—polysialic acid (PSA) and human natural killer cell epitope epitope (HNK-1)—that have been independently shown to encourage nerve regeneration and axonal targeting. Our novel biomaterial was used to bridge a critical gap size (5 mm) in a mouse femoral nerve injury model. Functional recovery was assessed using gait and hind limb extension, and was significantly better in all glycomimetic peptide-coupled collagen conditions versus non-functional scrambled peptide-coupled collagen, native collagen, and saline controls. Analysis of cross-sections of the regenerated nerve demonstrated that hydrogels coupled with the PSA glycomimetic, but not HNK, had significant increases in the number of myelinated axons over controls. Conversely, hydrogels coupled with HNK, but not PSA, showed improvement in myelination. Additionally, significantly more correctly projecting motoneurons were observed in groups containing coupled HNK-1 mimicking peptide, but not PSA mimicking peptide. Given the distinct morphological outcomes between the two glycomimetics, our study indicates that the enhancement of recovery following peripheral nerve injury induced by PSA- and HNK-functionalized collagen hydrogels likely occurs through distinct mechanisms.

Keywords

Peripheral nerve regeneration; PSA; HNK; Glycomimetics; Collagen

*Corresponding author. Tel.: +1 848 445 6589; fax: +1 732 445 3753. Shreiber@rci.rutgers.edu (D.I. Shreiber). **Corresponding author. Center for Neuroscience, Shantou University Medical College, 22 Xin Ling Road, Shantou 515041, China. Tel.: +86 754 8890 0276; fax: +86 754 8890 0236. schachner@stu.edu.cn (M. Schachner).

1. Introduction

Despite significant progress in encouraging the regrowth of peripheral nervous system (PNS) axons across large gap sizes, functional outcomes remain substantially sub-optimal. Research and development of regenerative strategies have primarily addressed means of preventing unwanted ingrowth of fibrous scar tissue, providing mechanical and trophic support for neural components, and presenting structural cues for longitudinally oriented neurite outgrowth [1,2]. Each of these approaches attempts to overcome obstacles in the injury microenvironment that are largely viewed as the primary sources of functional failure. There is now increasing evidence to suggest that the malrouted reinnervation of neurites towards inappropriate targets also contributes to poor functional outcome [3] as well as muscle weakness, lifelong pain, and inappropriate reflex arcs [4]. Although many of the incorrect neural circuits are pruned during the regeneration process, their growth is effectively wasted. Despite the potential benefits of improving the quality of end target reinnervation following PNS injury, regenerative strategies that specifically address axon targeting are rare.

Growth cones respond to many local cues that regulate axonal guidance and targeting during development. Though not as well studied, the post-PNS injury microenvironment can also direct regenerating axons. One particularly interesting example is a phenomenon known as preferential motor reinnervation (PMR), which has been shown to increase the efficiency of synaptic reconnection of motor axons. Immediately following injury, proximal neurites grow randomly towards the distal end connecting with both motor and sensory targets. However, as reinnervation continues, the number of motor axons connecting with their appropriate motor targets increases [5–8]. Although the mechanisms that govern PMR are not clearly understood, it is generally accepted that trophic factors, including recognition molecules, that can be expressed locally in the spinal cord and very distally from the injury site are largely involved.

Two glycans, polysialic acid (PSA) and an epitope first discovered on human natural killer cells (HNK-1), have been implicated in acceleration of regrowth and PMR following nerve damage. Franz et al. demonstrated that the level of expression of PSA dramatically increases in motoneurons following nerve injury compared to that from uninjured-motoneurons. When this upregulation is enzymatically interrupted following injury, PMR is significantly inhibited [9]. Among myelinating Schwann cells, HNK-1 is predominantly expressed on those that are associated with motor axons, implicating the modality specific role of this glycan in the PNS [10,11]. Martini et al. demonstrated that the presence of HNK-1 increases moto-neuron outgrowth, but does not affect sensory neuron outgrowth invitro [12]. Further, following injury, only myelinating Schwann cells that had been previously associated with motor axons re-express HNK-1. Sensory-associated Schwann cells do not produce the glycan even after prolonged exposure to motor axons [11]. Eberhardt et al. showed that electrical stimulation of damaged femoral nerves in the PNS increased HNK-1 expression, which correlated to an increase in muscle reinnervation and functional recovery [13].

Despite their functional roles, difficulties in synthesis and/or poor stability in vivo have limited the therapeutic use of glycans. Alternative strategies to upregulate these molecules following injury, such as electrical stimulation of nerve stumps and implantation of genetically modified cells, have yielded promising results [13–16]. However, the likelihood of their clinical translation is limited. Recent advances in analytic techniques have allowed the discovery of glycomimetic peptides, which provides new opportunities to exploit this class of therapeutic targets. These molecular mimics generally retain the functionality of their carbohydrate counterparts, with the added potential benefits of ease of production, increased stability, and reduced cost [17,18].

Recently, peptide mimics of PSA and HNK-1 have been isolated using phage display screening [19,20]. These glycomimetics have been used successfully in small gap repair of peripheral nerve injury when presented in soluble form in both mouse [21,22] and non-human primate models [23], but their use in more challenging injury models requires increasing the lifetime of their presentation. To this end, we have coupled the glycomimetics to a type I collagen backbone, thereby providing well-controlled, sustained presentation of these cues. Collagen hydrogels provide a useful intraluminal filling as collagen is easily modified, resorbable, and porous. Further, cells can stably bind to collagen via integrins, which leads to regeneration-conducive rearrangements of cellular activities via signal transduction and cytoskeletal functions. Collagen alone has previously been shown to be efficacious in improving regeneration following peripheral nerve injury [24,25]. In its hydrogel form, collagen provides a highly controlled environment for nerve cells to grow by providing both mechanical and biological support for neuritogenesis [26]. In a previous study, we confirmed the in vitro bioactivity of type I collagen hydrogels that were functionalized with PSA and HNK-1 glycomimetics and showed that the molecules retain their modality specific responses towards neural cells after conjugation [27].

Herein, we evaluate the utility of the glycomimetic peptide-coupled collagen for critical gap peripheral nerve injuries. We use the femoral nerve injury model (FNI) with a critical gap size of 5 mm, which exceeds the previously used gap size of 2 mm. The FNI model, first introduced by Brushart to understand the mechanism of PMR [5–7], is a particularly well-suited experimental paradigm to study morphological and functional measures of recovery. The femoral nerve begins as a mixed nerve containing sensory and motor axons, and then bifurcates into the sensory saphenous branch and the motor/sensory quadriceps branch. This modality-exclusive branching allows for evaluation of the targeting efficiency, as the bifurcation provides an anatomical decision point for regenerating motor axons; correctly targeting motor axons must choose the quadriceps branch. Thus, in addition to standard scores of morphological and functional recovery, we can evaluate PMR using retrograde labeling techniques (Fig. 1).

2. Methods

2.1. Functionalization of collagen

From sequences identified previously as functional glycomimetics [19,20], one linear glycomimetic peptide was selected for HNK-1 (FLHTRLFV, MW: 1032.24) and for PSA (SSVTAWTTG, MW: 908.97). A scrambled version of the HNK-1 peptide (TVFHFRLL) served as a control. All peptides were acquired from a commercial vendor (Genscript, Piscataway, NJ).

Peptides were covalently conjugated onto oligomeric type I collagen using the heterobifunctional crosslinker 1-ethyl-3-(3-dimethylaminopropyl) carbodiimide (EDC) as previously described [28]. Briefly, fetal calf type I collagen (EPC, Owensville, MO) was reconstituted to 3 mg/ml in 0.02 N acetic acid to make an oligomeric collagen solution. To activate carboxyl groups, 2 mg of peptide were dissolved in 2 ml of MES buffer (Fluka) containing 1 mM EDC (Pierce) and reacted for 15 min at 37 °C. Following this incubation, the activated peptide was added to 5 ml oligomeric collagen solution and rotated overnight at 4 °C. The peptide/collagen solution was dialyzed overnight to remove unattached peptide with two dialyzate changes. Finally, the purified solution was lyophilized and reconstituted to 3 mg/ml in 0.02 N acetic acid. In a previous study using this conjugation technique, we confirmed that the resulting coupling efficiency is between 50 and 60%, which translates to 200–240 μg of coupled peptide per ml collagen. Additionally, the grafting process does not significantly change the mechanical properties, fiber diameter, or fiber density of the hydrogel [28].

2.2. Preparation of conduits

Collagen hydrogels at 2.0 mg/ml were prepared as previously described [29]. Native or functionalized oligomeric collagen solutions at 3 mg/ml were neutralized on ice using solutions in the following ratios: 2% 1 M Hepes (Fluka), 14% 0.1 N NaOH, 10% 10X Minimum Essential Medium (Sigma), 5.2% M199 (Sigma), 0.1% penicillin/streptomycin (P/S; Sigma), 1% L-glutamine (L-glut; Sigma), 67.7% native or peptide-functionalized collagen. The final concentration of coupled peptide within the hydrogel was between 130 and 160 μg per ml collagen, which was similar to the effective doses given in solution in previous in vivo studies [21,22]. (For simplicity, hydrogels coupled with the HNK-1 glycomimetic peptide are referred to as HNK-coupled hydrogels, and hydrogels coupled with the PSA glycomimetic peptide are referred to as PSA-coupled hydrogels.) For composite PSA/HNK-coupled hydrogels containing both of the glycomimetics, 33.85% of each of the HNK- and PSA-coupled collagen solutions were neutralized using the formulation above. Glycomimetic peptide-coupled hydrogels refers to the hydrogels coupled with PSA, HNK, or PSA/HNK.

Polyethylene (PE) tubes (0.6 mm ID/1 mm OD) were pre-cut to a 5.5 mm length and UV sterilized. Native and functionalized collagen solutions were injected in excess to ensure complete void filling into PE tubes using a 22 gauge syringe. The tubes were incubated at 37 °C to allow self-assembly of the hydrogel. Control tubes were filled with a sterile PBS solution immediately prior to implantation.

2.3. Animals and surgical procedure

All procedures were conducted in accordance with approved protocols from the Institutional Animal Care and Use Committee (IACUC). Ten week old C57/B6 female mice (Taconic Farms) were heavily anesthetized by intraperitoneal injections of a ketamine (80 mg/kg) and xylazine (12 mg/mg) mixture. The surgical area was shaved and cleaned with a Betadine scrub and alcohol. The left femoral nerve was exposed, and a nerve transection was performed at a distance about 3 mm proximal to the bifurcation of the nerve. The cut ends of the nerve were inserted into the pre-filled PE tube fixed with single epineural 10-0 nylon stitches (Ethicon) so that a 5 mm gap was present between the proximal and distal stump. The incised skin was closed with wound clips, which were then removed one week post-surgery.

2.4. Measures of functional recovery

Injury to the femoral nerve proximal to the point of bifurcation deinnervates the quadriceps muscle. During gait, the quadriceps muscle maintains knee extension in single support phases thereby allowing the contralateral leg to swing forward. Given this distinct biomechanical role, Irintchev et al. [27] developed an approach to quantify the kinematic effects of this type of injury. We used two of Irintchev's defined parameters to evaluate functional recovery: the foot base angle (FBA) and the protraction limb ratio (PLR).

2.4.1. Foot base angle—Following femoral nerve injury, impaired bending of the knee results in plantar flexion of the ankle joint during load bearing movements. With the classical beam-walk test, this response can be quantified by measuring the angle at which the sole of the hindpaw meets the surface when the contralateral leg is lifted, termed the foot base angle (FBA) [30]. As shown in Fig. 2, during complete load bearing movements, the hindpaw is externally rotated in the transverse plane in intact animals. However, one week following injury, the hindpaw is externally rotated due to a loss in quadriceps innervation. Animals (n = 10–12 per experimental condition) were trained to walk across a 1 m long wooden beam towards their home cage. Mice were filmed from the rear using a high speed camera (A602fc, Basler) prior to injury and at 1, 8, 12, and 15 weeks following injury. The

locomotion videos were analyzed using single frame motion analysis (SFMA) using SimiMotion (SIMI Reality Motion Systems). The FBA was measured at a specific stage of the gait cycle where the contralateral leg was at its highest point, which is when the injured leg bears the most weight. The FBA was determined by dividing the left hind sole into two halves and measuring the angle of that line with the horizontal.

2.4.2. Protraction limb ratio—The protraction limb ratio (PLR) is measured using a pencil grip test and provides analysis of voluntary movement and proprioceptive ability that is more dependent on supraspinal control compared to gait. Additionally, these pursuits do not require weight support. At weeks 0, 1, 8, and 15, a subset of animals (n = 6–7 per experimental condition) were held by their tail and allowed to grab a pencil fixed vertically below them with their forelimbs. The hind limbs will alternate between flexion and extension in an attempt to grab the pencil tip. As shown in Fig. 2, frames during the extension phase were used to measure the PLR, defined as the distance between the anus and the longest digit on the paw [30]. Before injury, limb extension is symmetric and the ratio of the extension for the right/left hind limb is approximately 1. After injury, this ratio increases due to the inability for the injured hind limb to extend completely. As successful regeneration proceeds, the ratio approaches unity once again.

2.4.3. Recovery index calculation—The recovery index (RI) was used as a relative score of functional recovery normalized to the week one FBA or PLR. The RI was calculated as a percent using the following equation:

$$\mathrm{RI}=\frac{X_{\mathrm{reinn}}-X_{\mathrm{den}}}{X_{\mathrm{pre}}-X_{\mathrm{den}}}\times 100$$

where X_{pre}, X_{den}, X_{reinn} were the values of the FBA or PLR prior to injury, one week following transaction, and at 15 weeks post injury, respectively [30].

2.5. Retrograde labeling and analysis

Fifteen weeks post-injury, a subset of mice underwent a secondary surgery to introduce retrograde labels into the branches of the femoral nerve (Fig. 1). Under ketamine/xylazine-induced anesthesia (see above), the left femoral nerve was exposed. The quadriceps and saphenous branches were transected approximately 5 mm distal to the point of bifurcation. Two fluorescent retrograde tracers were applied in crystal form to the proximal nerve stumps: 10,000 MW dextran labeled with Alexa Fluor 488 in the saphenous branch, and 10,000 MW dextran labeled with Alexa Fluor 546 in the quadriceps branch (Invitrogen). After 30 min, excess dye was removed, nerve stumps were rinsed with PBS, and the incision was closed with wound clips. The labels were allowed to passively traverse back into the spinal cord for one week. Animals were then heavily anaesthetized and perfused through the left ventricle with 4% paraformaldehyde. The lumbar spinal cord was removed and post-fixed overnight in 4% paraformaldehyde and then immersed in a 20% sucrose-saline solution. The entire lumbar enlargement was then serially sectioned transversely at a thickness of 50 μm. All labeled motoneurons fell within a stack of approximately 40 serial cross-sections, and each of these sections generally contained 1–5 retrograde-labeled motoneurons. To prevent double-counting of labeled motoneurons, sections spaced 250 μm apart were examined (between 7 and 10 serial cross-sections per animal) with an inverted epifluorescence microscope (Olympus IX81) for labeled motoneurons using a 20X objective. Labeled motoneurons were only visible in the ventral horn, the motoneuron rich region of the spinal cord. The number of correctly targeted, Alexa Fluor 546+ motoneurons

and the number of incorrectly targeted, Alexa Fluor 488+ motoneurons were counted for each animal.

2.6. Histomorphometry of regenerated nerve

In addition to the lumbar spinal cord, the implanted conduits were also removed post-sacrifice. Samples were post fixed overnight in 4% paraformaldehyde and then immersed in a 20% sucrose-saline solution. A 2 mm segment from the middle of the regenerated nerve was treated with 1% osmium tetroxide solution in 0.1 M sodium cacodylate buffer for 1 h at room temperature. Osmium fixed samples were then dehydrated, embedded in an epoxy resin, and cut into 1 μm-thick cross-sections. Sections were counter-stained with 1% toluidine blue in 1% borax in distilled water to enhance contrast. Composite images were captured in bright field using a 100X oil immersion objective. Excised nerves with preserved epineurial sheaths (n = 8–10 per experimental condition) were used to manually count the number of myelinated axons per regenerated nerve cross-section using Image J (NIH). These samples were also used to calculate the percent nerve tissue regeneration by dividing the area of nerve tissue regeneration by the total tissue area. The area of nerve tissue regeneration was defined as the fascicular area containing myelinated axons. Within a subset of these nerves (n = 6 per experimental condition), for each myelinated axon, the mean orthogonal diameter of the axon and of the fiber (axon + myelin sheath) was measured. The mean orthogonal diameter was defined as the average of the length the longest axis of the axon and the perpendicular of that line. The g-ratio, a measure of the quality of myelination, was then calculated as the ratio of the axon-to-fiber diameter. The g-ratio scores were then binned with respect to axon size using a 1 μm bin size [31].

2.7. Statistical analysis

The study was designed to allow comparison of saline and hydrogel treated conditions, glycomimetic peptide-coupled and non-glycomimetic treated conditions, and within glycomimetic peptide-coupled treated conditions. Variance analysis using a one-way ANOVA was used followed by post-hoc planned comparisons with Tukey's test. Differences were considered significant at $p < 0.05$.

3. Results

3.1. Functional recovery

3.1.1. Foot base angle (FBA)—Injury to the femoral nerve results in abnormal external rotation of the hindpaw, which can be quantified using the FBA (Fig. 2). Prior to injury, the FBA did not differ significantly among groups, and was approximately 68° (Fig. 3A). One week post-injury, this angle increased to approximately 99°, and was again not significantly different among groups. At eight, twelve, and fifteen weeks post-injury, the angle for all collagen hydrogel treated groups decreased towards the original values, and significantly outperformed saline treated groups ($p < 0.0001$ for all weeks). Glycomimetic peptide-coupled collagen outperformed native and scrambled peptide-coupled collagen at all measured time points ($p = 0.00141$, $p < 0.0001$, and $p = 0.00011$, respectively). However, no significant differences were found among the glycomimetic peptide-coupled groups or between native and scrambled peptide-coupled collagen at any of these time points.

The recovery index (RI) was used to normalize the degree of functional recovery to the injury at week one (Fig. 3B). At eight, twelve, and fifteen weeks post-injury, the RI for collagen hydrogel treated groups was significantly greater than for saline treated groups ($p = 0.00017$, $p = 0.00023$, and $p < 0.0001$, respectively). Within hydrogel treated groups, the RI for glycomimetic peptide-coupled collagen was significantly greater than for native and scrambled peptide-coupled collagen ($p = 0.00518$, $p = 0.0006$, and $p < 0.0001$, respectively).

At eight weeks post-injury, no significant differences in the RI were noted between scrambled peptide- and glycomimetic peptide-coupled groups. However at twelve and fifteen weeks, glycomimetic peptide-coupled collagen significantly outperformed scrambled peptide-coupled collagen ($p = 0.02321$ and $p = 0.00197$, respectively). Once again, no significant differences were found among glycomimetic peptide-coupled groups or between native and scrambled peptide-coupled groups at any of these time points.

3.1.2. Protraction limb ratio (PLR)—The PLR quantifies the animal's ability to grasp a stationary item fixed below it. More so than ground locomotion, these target-reaching, voluntary movements are generally dependent on supra-spinal and proprioceptive involvement. Following femoral nerve injury, the quadriceps cannot fully extend the knee, which results in an impaired ability to complete this pursuit (Fig. 2). The ipsilateral and contralateral extensions are compared to generate the PLR.

The PLR increased from approximately 1.0 pre-injury to approximately 1.45 post-injury, with no statistically significant differences among the treatment groups (Fig. 4A). At eight and fifteen weeks post injury, the PLR for saline groups was significantly higher than for hydrogel treated groups ($p = 0.00121$ and $p < 0.0001$, respectively). However, there were no statistically significant differences noted at either of these time points among collagen hydrogel treated groups. Based on the RI (Fig. 4B), collagen hydrogel treated groups outperformed saline treated animals at eight and fifteen weeks post-injury ($p = 0.00119$ and $p < 0.0001$, respectively). No significant differences were found among glycomimetic peptide-coupled groups or between native and scrambled peptide-coupled groups at either eight or fifteen weeks post-injury.

3.2. Morphological analysis

Histological evaluation of osmium tetroxide stained nerve cross-sections showed myelinated axons in all hydrogel treated groups. However, 4 out of 11 saline treated animals had few (<5) to no distinguishable axons (Fig. 5A–B). As shown in Fig. 5C, statistical analysis of axon numbers revealed significantly more axons in hydrogel treated groups than saline ($p = 0.00106$). Within hydrogel conditions, PSA-coupled hydrogels contained significantly more axons than hydrogels without the coupled PSA mimicking peptide ($p = 0.0153$). HNK-coupled hydrogels did not show significant differences in axon count when compared to hydrogels without the coupled HNK-1 mimicking peptide. As shown in Fig. 5D, all hydrogel treated conditions had a greater percent of regeneration compared to saline treated animals ($p = 0.01705$). There were no statistically significant differences in percentage of nerve regeneration among hydrogel treated groups.

The distribution of myelin within regenerated nerves was analyzed by quantifying the g-ratio, which is the ratio of the axon-to-fiber diameter (Fig. 6). A smaller g-ratio represents an increase in the amount of myelin surrounding the axon. G-ratios were binned with respect to axon size and then tested for statistical significance. In general, HNK-coupled hydrogels yielded the smallest g-ratio while other hydrogels did not differ significantly across axon sizes. For simplicity, the discussion below is restricted to HNK-coupled hydrogels. For a complete statistical analysis of groups tested, the reader is referred to Supplementary Table 1.

Within axons up to 4 μm in diameter, HNK-coupled hydrogels yielded significantly lower g-ratios when compared to all other injury conditions ($p < 0.01$). Between 4 and 5 μm, HNK-coupled hydrogels had significantly lower g-ratios than all other hydrogel treated groups but were not statistically significant different from saline treated nerves or intact, unoperated nerves ($p < 0.01$). Finally, nerves treated with HNK-coupled hydrogels were not significantly different than other regenerated nerves for axons larger than 5 μm. For these

larger axons (>5 μm), intact nerves yielded significantly lower g-ratios compared to all regenerated nerves ($p < 0.0001$). Notably, mean g-ratios of all regenerated nerves fell between 0.6 and 0.8, which has been shown to be physiologically healthy values for nerve conduction [32].

3.3. Retrograde labeling

To assess the effect of the coupled glycomimetics on targeting efficiency, different fluorescently tagged retrograde labels were introduced into the quadriceps and saphenous branch 15 weeks post injury (Fig. 1). One week following introduction of the dyes, animals were sacrificed and spinal cords were excised for motoneuron counts (Fig. 7A). Statistical evaluation of motoneuron counts revealed significantly more correctly labeled motoneurons in hydrogel treated groups versus saline ($p = 0.01341$; Fig. 7B). Within hydrogel-treated groups, HNK-coupled hydrogels contained significantly more correctly labeled motoneurons than hydrogels without the HNK-1 mimicking peptide ($p = 0.02$). No significant differences were noted between hydrogels with or without the coupled PSA mimicking peptide. No statistically significant differences were found between conditions with regard to numbers of incorrectly labeled motoneurons or the total number of labeled motoneurons (correct and incorrect).

4. Discussion

Despite the innate regenerative potential of the PNS, functional recovery remains incomplete with increasing severity of injury. This has been attributed to a number of reasons including the local inflammatory response, ingrowth of fibrous scar tissue, lack of mechanical support for emerging neurites, and more recently the malrouted regrowth of axons. We have previously shown that covalent conjugation of glycomimetic HNK-1 and PSA peptides to type I collagen results in neural cell type-specific responses in vitro [27]. Given these unique, modality-defined effects, we investigated the potential for glycomimetic functionalized collagen to promote axonal regeneration and targeting in a challenging, 5 mm gap size femoral nerve injury model. While these peptides have previously been shown to be efficacious in smaller gap sizes [22,23,33], this is the first successful study utilizing the peptide mimics within a critical gap.

Following implantation of a polyethylene tube filled with glycomimetic functionalized collagen after injury, we observed significant improvement in functional and morphological recovery as summarized in Table 1. These positive effects are due to the structural similarity between the glycomimetic peptides and their respective carbohydrate epitope. Previous studies have shown that the peptides have specific binding affinity for anti-PSA and anti-HNK-1 antibodies [19,20,33]. Additionally, the scrambled peptide-coupled collagen did not elicit any more benefit than native collagen, which also indicates that these effects are sequence specific.

4.1. Utility of the femoral nerve injury model

The femoral nerve injury paradigm was used to test the in vivo efficacy of our modified collagen hydrogels, as it is particularly well suited to assess functional and morphological recovery [34]. Although the sciatic nerve model is most widely used for peripheral nerve injury, it has been criticized as having limited reliability in quantifying functional recovery. In the sciatic model, a single behavior is generally used to represent the relative contributions of numerous muscles affected by sciatic nerve transection. Further, return of function is often measured using ink prints of the hindpaw. This approach is frequently difficult to interpret due to smearing, incomplete steps, and self-mutilation which limit the precision of this paradigm [35–37]. In contrast, the femoral model allows for objective,

sensitive measurement of quadriceps reinnervation over the course of regeneration using FBA and PLR scores.

Perhaps the most interesting use of the femoral nerve paradigm stems from its unique anatomy that allows for quantitative evaluation of motoneuron targeting. Near the inguinal ligament, the mixed femoral nerve divides into two branches of similar diameters - the sensory saphenous branch and the mixed quadriceps branch (Fig. 1). If the femoral nerve is injured prior to the point of bifurcation, regenerating motor axons have equal opportunity to grow into the incorrect saphenous branch or the correct quadriceps branch. When PMR occurs, more motor axons will be located in the correct pathway as assessed with retrograde labeling. Collectively, the model allows for insights into the mechanisms underlying motor axon targeting and evaluation of methods to improve its propensity of occurring.

4.2. Collagen as an intraluminal filler

The present study demonstrates that native and grafted collagen hydrogels provide significant functional and morphological benefits compared to saline filled conduits. These findings are in agreement with increasing evidence that suggests that a nerve guidance conduit for longer, clinically relevant gap sizes will likely involve optimization of the inner lumen in addition to improving the chemistry of the outer tube [38]. The intraluminal filling serves to replace the fibrin cable which often fails to form in the case of larger injuries [39]. In doing so, the matrix provides a supportive substrate for the ingrowth of Schwann cells and regenerating axons [40].

4.3. Glycomimetic functionalized collagen hydrogels

The greatest overall improvement in functional and morphological recovery was observed in groups treated with glycomimetic peptide-functionalized collagen. By covalent conjugation of the glycomimetics to the collagen backbone, it is possible that peptidase-mediated degradation is limited and time of local availability is increased. Further, since PSA and HNK-1 glycans in their native configuration are tethered to the extracellular matrix or presented on the cell surface in vivo, the mode of presentation may be more physiologically relevant when compared to administration in their soluble forms.

Functional recovery was assessed using two methods: the FBA and PLR. When measured using the FBA, glycomimetic peptide-coupled hydrogels significantly outperformed non-glycomimetic peptide-coupled hydrogels. On the other hand, there were no significant differences noted between any of the hydrogel treated groups when measured using the PLR. The differences in functional outcomes between these two tests are likely related to the importance of quadriceps reinnervation in the successful completion of the task. The PLR is a non-weight bearing pursuit and therefore may not have adequate sensitivity to negotiate differences in quadriceps function between treatment groups. Additionally, other muscles involved in lower limb extension, including the biceps femoris, may provide compensation during the reaching pursuit. The FBA quantifies changes during the stance phase of the gait cycle where the affected quadriceps muscle bears body weight. Other muscle groups would provide minimal compensation as the quadriceps is solely responsible for the knee extension. The functional scores at eight weeks post injury provide evidence that the FBA may be a more appropriate metric to assess changes in quadriceps rein-nervation. Whereas the PLR RI scores for the hydrogel treated groups were between 60 and 80%, the FBA RI scores for the FBA were between 20 and 40%. It is unlikely that at this time point the quadriceps has up to 80% successful reinnervation as suggested by the PLR scores. However, it should be noted that the PLR may provide an early screening tool to assess quadriceps reinnervation.

Although both PSA- and HNK-coupled hydrogels resulted in similar functional recovery, the morphological outcomes indicate that distinct cellular mechanisms may be involved (Table 1). Mice treated with PSA-coupled collagen had significantly higher axon counts, whereas mice treated with HNK-coupled collagen showed increased myelin and motor axon targeting compared to saline and other hydrogel-treated conditions. The different outcomes in the morphological parameters add evidence that the mode of action of the peptides is likely related to their functions as glycan homologs.

Following peripheral nerve injury, axons will extend several exploratory collateral sprouts towards distal nerve branches. Franz et al. have demonstrated that PSA is an important determinant of this phenomenon [9]. PSA is generally found tethered to the neural cell adhesion molecule (NCAM), and has been suggested to promote axon regrowth by sterically limiting heterophilic and homophilic NCAM interactions [41]. When enzymatically removed or genetically interrupted, PSA-deficient mice have significantly reduced axon numbers within regenerated nerve cables [9]. These findings are in agreement with our results, which show an increase in axon count in nerves treated with PSA-coupled collagen. The differences in axon count are not related to an increase in the area of regeneration, but reflect an increase in the density of axonal sprouts. Since the total number of labeled motoneurons was not significantly different between hydrogel treated groups, it is likely that the increase in axon count reflects an increase in collateral sprouts and not an increase in motoneurons. Thus, these axonal projections likely create more chances for the regenerating axons to reach their appropriate target and may account for an increase in locomotor recovery. We did not observe improvement in axonal targeting underlying PMR with PSA, which is consistent with previous work from Mehanna et al. [21].

The increased myelin production resulting from incorporation of the HNK-1 mimicking peptide is also in agreement with studies on the function of its glycan counterpart. In the canine, HNK-1 was recently found to be associated with myelinating Schwann cells with limited-to-no expression on non-myelinating Schwann cells, which supports the view that the glycan is related to myelin production [42]. Interestingly, Simova et al. demonstrated that soluble administration of the HNK-1 mimicking peptide resulted in an increase in HNK-1 expression in the quadriceps branch of the injured mouse femoral and an increase in myelin thickness [22]. Although evaluating changes in myelin production as a function of axon phenotype was beyond the scope of this study, future work will explore if introduction of HNK-coupled hydrogels differentially affects myelination of motor versus sensory axons.

The targeting results with HNK-coupled collagen are in agreement with previous results in the 2 mm gap paradigm in mouse and monkey where the peptide was presented in solubilized form [22,23]. In vivo, HNK-1 has an unusual, highly specific expression pattern on mouse motor-associated Schwann cells [11], and its expression is increased following administration of the peptide [22]. This may lead to a more permissive environment for proliferating Schwann cells and regenerating motor axons and ‘prime’ them for other downstream trophic cues. More specifically, recent evidence has suggested that the HNK-1 glycan causes activation of the receptor for the advanced glycation end products (RAGE) through its interaction with HMGB1 (amphoterin). The activation of this pathway leads to increased neurite outgrowth and survival, and impairment of RAGE signaling significantly reduces nerve regeneration [43–45]. Other molecular mechanisms underlying the observed effects could be due to the ability of HNK-1 to bind to laminin [46].

Given these distinct responses, using a combination of the two glycomimetics could potentially provide synergistic benefit. In this study, however, we did not see any significant increase in functional or morphological improvement from presentation of both of these cues simultaneously. We speculate that this may be due to an inadequate concentration of

the conjugated peptides. To maintain equal total peptide concentration between coupled collagen conditions, the PSA/HNK-coupled hydrogels were made in 50/50 ratios. Future work will evaluate varied concentrations of PSA/HNK-coupled hydrogels to find optimal concentrations using in vitro methods. The ratios which elicit maximal benefit can then be translated to in vivo use. It is also possible that functional recovery was maximized for this time point or this model. Thus, future work will evaluate the performance of the materials in larger animals, later time points, and other nerve injury models. In addition to peptide grafting, collagen is amenable to other higher order modifications including gradient generation [47] and longitudinal fiber alignment [48,49]. Future studies will evaluate the benefit of introducing structural and haptotactic anisotropy to our biomaterial.

5. Conclusion

The peptide glycomimetics of PSA and HNK-1 represent interesting target molecules to improve the efficiency of synaptic reconnection. In this study, the efficacy of glycomimetic-functionalized collagen hydrogels as a strategy for repair following peripheral nerve injury (PNI) is described. Although both PSA- and HNK-coupled hydrogels encouraged functional recovery following femoral nerve transection, the distinct morphological outcomes indicate the peptides likely function through different mechanisms related to their glycan homolog. Specifically, PSA-coupled collagen improved axon number, whereas HNK-coupled collagen improved motoneuron targeting and myelination of axons. Collectively, this study represents a biomaterial approach at improving the efficiency of synaptic reconnection and functional recovery following PNI.

Supplementary Material

Refer to Web version on PubMed Central for supplementary material.

Acknowledgments

Funding for these studies was provided by the National Institutes of Health (NIH 1R21EB009245-01A1) and US Army contract #W81XWH-04-2-0031, and fellowships from the Rutgers-UMDNJ Biotechnology Training Program (NIH Grant Number 5T32GM008339-20), the National Science Foundation (NSF DGE 0801620, IGERT on the Integrated Science and Engineering of Stem Cells), and the Aresty Research Center for Undergraduates. MS is a New Jersey Professor of Spinal Cord Research. We confirm that all studies involving experimental animals were conducted under the ethical approval of all relevant bodies.

Appendix A. Supplementary material

Supplementary material associated with this article can be found, in the online version, at http://dx.doi.org/10.1016/j.biomaterials.2012.08.018.

References

1. Huang YC, Huang YY. Biomaterials and strategies for nerve regeneration. Artif Organs. 2006; 30(7):514–22. [PubMed: 16836732]
2. Hudson TW, Evans GR, Schmidt CE. Engineering strategies for peripheral nerve repair. Clin Plast Surg. 1999; 26(4):617–28. [PubMed: 10553217]
3. Sumner AJ. Aberrant reinnervation. Muscle Nerve. 1990; 13(9):801–3. [PubMed: 2233866]
4. Sunderland, S. Nerves and nerve injuries. 2. New York: Churchill Livingstone; 1978.
5. Brushart TM, Seiler WAt. Selective reinnervation of distal motor stumps by peripheral motor axons. Exp Neurol. 1987; 97(2):289–300. [PubMed: 3609213]
6. Brushart TM. Preferential reinnervation of motor nerves by regenerating motor axons. J Neurosci. 1988; 8(3):1026–31. [PubMed: 3346713]

7. Brushart TM. Motor axons preferentially reinnervate motor pathways. J Neurosci. 1993; 13(6): 2730–8. [PubMed: 8501535]
8. Madison RD, Archibald SJ, Brushart TM. Reinnervation accuracy of the rat femoral nerve by motor and sensory neurons. J Neurosci. 1996; 16(18):5698–703. [PubMed: 8795625]
9. Franz CK, Rutishauser U, Rafuse VF. Polysialylated neural cell adhesion molecule is necessary for selective targeting of regenerating motor neurons. J Neurosci. 2005; 25(8):2081–91. [PubMed: 15728848]
10. Martini R, Bollensen E, Schachner M. Immunocytological localization of the major peripheral nervous-system glycoprotein P0 and the L2/HNK-1 and L3 carbohydrate structures in developing and adult-mouse sciatic-nerve. Dev Biol. 1988; 129(2):330–8. [PubMed: 2458286]
11. Martini R, Schachner M, Brushart TM. The L2/HNK-1 carbohydrate is preferentially expressed by previously motor axon-associated schwann cells in reinnervated peripheral nerves. J Neurosci. 1994; 14(11):7180–91. [PubMed: 7525896]
12. Martini R, Xin Y, Schmitz B, Schachner M. The L2/HNK-1 carbohydrate epitope is involved in the preferential outgrowth of motor neurons on ventral roots and motor nerves. Eur J Neurosci. 1992; 4(7):628–39. [PubMed: 12106326]
13. Eberhardt KA, Irintchev A, Al-Majed AA, Simova O, Brushart TM, Gordon T, et al. BDNF/TrkB signaling regulates HNK-1 carbohydrate expression in regenerating motor nerves and promotes functional recovery after peripheral nerve repair. Exp Neurol. 2006; 198(2):500–10. [PubMed: 16460731]
14. Luo J, Bo X, Wu D, Yeh J, Richardson PM, Zhang Y. Promoting survival, migration, and integration of transplanted schwann cells by over-expressing polysialic acid. Glia. 2010
15. El Maarouf A, Petridis AK, Rutishauser U. Use of polysialic acid in repair of the central nervous system. Proc Natl Acad Sci U S A. 2006; 103(45):16989–94. [PubMed: 17075041]
16. Franz CK, Rutishauser U, Rafuse VF. Intrinsic neuronal properties control selective targeting of regenerating motoneurons. Brain. 2008; 131(Pt 6):1492–505. [PubMed: 18334536]
17. Magnani JL, Ernst B. Glycomimetic drugs – a new source of therapeutic opportunities. Discov Med. 2009; 8(43):247–52. [PubMed: 20040279]
18. Ernst B, Magnani JL. From carbohydrate leads to glycomimetic drugs. Nat Rev Drug Discov. 2009; 8(8):661–77. [PubMed: 19629075]
19. Simon-Haldi M, Mantei N, Franke J, Voshol H, Schachner M. Identification of a peptide mimic of the L2/HNK-1 carbohydrate epitope. J Neurochem. 2002; 83(6):1380–8. [PubMed: 12472892]
20. Torregrossa P, Buhl L, Bancila M, Durbec P, Schafer C, Schachner M, et al. Selection of poly-alpha 2,8-sialic acid mimotopes from a random phage peptide library and analysis of their bioactivity. J Biol Chem. 2004; 279(29):30707–14. [PubMed: 15131117]
21. Mehanna A, Mishra B, Kurschat N, Schulze C, Bian S, Loers G, et al. Polysialic acid glycomimetics promote myelination and functional recovery after peripheral nerve injury in mice. Brain. 2009; 132:1449–62. [PubMed: 19454531]
22. Simova O, Irintchev A, Mehanna A, Liu J, Dihne M, Bachle D, et al. Carbohydrate mimics promote functional recovery after peripheral nerve repair. Ann Neurol. 2006; 60(4):430–7. [PubMed: 16958115]
23. Irintchev A, Wu MM, Lee HJ, Zhu H, Feng YP, Liu YS, et al. Glycomimetic improves recovery after femoral injury in a non-human primate. J Neurotrauma. 2011; 28(7):1295–306. [PubMed: 21463132]
24. Satou T, Nishida S, Hiruma S, Tanji K, Takahashi M, Fujita S, et al. A morphological study on the effects of collagen gel matrix on regeneration of severed rat sciatic nerve in silicone tubes. Acta Pathol Jpn. 1986; 36(2):199–208. [PubMed: 2422877]
25. Rosen JM, Padilla JA, Nguyen KD, Padilla MA, Sabelman EE, Pham HN. Artificial nerve graft using collagen as an extracellular-matrix for nerve repair compared with sutured autograft in a rat model. Ann Plast Surg. 1990; 25(5):375–87. [PubMed: 2175157]
26. Sundararaghavan HG, Monteiro GA, Firestein BL, Shreiber DI. Neurite growth in 3D collagen gels with gradients of mechanical properties. Biotechnol Bioeng. 2009; 102(2):632–43. [PubMed: 18767187]

27. Masand SN, Perron IJ, Schachner M, Shreiber DI. Neural cell type-specific responses to glycomimetic functionalized collagen. Biomaterials. 2012; 33(3):790–7. [PubMed: 22027596]
28. Monteiro GA, Fernandes AV, Sundararaghavan HG, Shreiber DI. Positively and negatively modulating cell adhesion to type I collagen via peptide grafting. Tissue Eng Part A. 2009
29. Shreiber DI, Barocas VH, Tranquillo RT. Temporal variations in cell migration and traction during fibroblast-mediated gel compaction. Biophys J. 2003; 84(6):4102–14. [PubMed: 12770913]
30. Irintchev A, Simova O, Eberhardt KA, Morellini F, Schachner M. Impacts of lesion severity and tyrosine kinase receptor B deficiency on functional outcome of femoral nerve injury assessed by a novel single-frame motion analysis in mice. Eur J Neurosci. 2005; 22(4):802–8. [PubMed: 16115204]
31. McCreery DB, Yuen TG, Agnew WF, Bullara LA. A quantitative computer-assisted morphometric analysis of stimulation-induced injury to myelinated fibers in a peripheral nerve. J Neurosci Methods. 1997; 73(2):159–68. [PubMed: 9196287]
32. Chomiak T, Hu B. What is the optimal value of the g-ratio for myelinated fibers in the rat CNS? A theoretical approach. PLoS One. 2009; 4(11):e7754. [PubMed: 19915661]
33. Mehanna A, Jakovcevski I, Acar A, Xiao M, Loers G, Rougon G, et al. Polysialic acid glycomimetic promotes functional recovery and plasticity after spinal cord injury in mice. Mol Ther. 2010; 18(1):34–43. [PubMed: 19826404]
34. Irintchev A. Potentials and limitations of peripheral nerve injury models in rodents with particular reference to the femoral nerve. Ann Anat. 2011; 193(4):276–85. [PubMed: 21481575]
35. Monte-Raso VV, Barbieri CH, Mazzer N, Yamasita AC, Barbieri G. Is the sciatic functional index always reliable and reproducible? J Neurosci Methods. 2008; 170(2):255–61. [PubMed: 18325595]
36. Shenaq JM, Shenaq SM, Spira M. Reliability of sciatic function index in assessing nerve regeneration across a 1 cm gap. Microsurgery. 1989; 10(3):214–9. [PubMed: 2796717]
37. Varejao AS, Melo-Pinto P, Meek MF, Filipe VM, Bulas-Cruz J. Methods for the experimental functional assessment of rat sciatic nerve regeneration. Neurol Res. 2004; 26(2):186–94. [PubMed: 15072638]
38. Bellamkonda RV. Peripheral nerve regeneration: an opinion on channels, scaffolds and anisotropy. Biomaterials. 2006; 27(19):3515–8. [PubMed: 16533522]
39. Zhao Q, Dahlin LB, Kanje M, Lundborg G. Repair of the transected rat sciatic nerve: matrix formation within implanted silicone tubes. Restor Neurol Neurosci. 1993; 5(3):197–204. [PubMed: 21551902]
40. Pfister LA, Papaloizos M, Merkle HP, Gander B. Nerve conduits and growth factor delivery in peripheral nerve repair. J Peripher Nerv Syst. 2007; 12(2):65–82. [PubMed: 17565531]
41. Johnson CP, Fujimoto I, Rutishauser U, Leckband DE. Direct evidence that neural cell adhesion molecule (NCAM) polysialylation increases intermembrane repulsion and abrogates adhesion. J Biol Chem. 2005; 280(1):137–45. [PubMed: 15504723]
42. Bock P, Beineke A, Techangamsuwan S, Baumgartner W, Wewetzer K. Differential expression of HNK-1 and p75(NTR) in adult canine schwann cells and olfactory ensheathing cells in situ but not in vitro. J Comp Neurol. 2007; 505(5):572–85. [PubMed: 17924534]
43. Chou DK, Zhang J, Smith FI, McCaffery P, Jungalwala FB. Developmental expression of receptor for advanced glycation end products (RAGE), amphoterin and sulfoglucuronyl (HNK-1) carbohydrate in mouse cerebellum and their role in neurite outgrowth and cell migration. J Neurochem. 2004; 90(6):1389–401. [PubMed: 15341523]
44. Rong LL, Trojaborg W, Qu W, Kostov K, Yan SD, Gooch C, et al. Antagonism of RAGE suppresses peripheral nerve regeneration. FASEB J. 2004; 18(15):1812–7. [PubMed: 15576484]
45. Fang P, Schachner M, Shen YQ. HMGB1 in development and diseases of the central nervous system. Mol Neurobiol. 2012; 45(3):499–506. [PubMed: 22580958]
46. Hall H, Liu L, Schachner M, Schmitz B. The L2/HNK-1 carbohydrate mediates adhesion of neural cells to laminin. Eur J Neurosci. 1993; 5(1):34–42. [PubMed: 8261088]
47. Sundararaghavan HG, Masand SN, Shreiber DI. Microfluidic generation of haptotactic gradients through 3D collagen gels for enhanced neurite growth. J Neurotrauma. 2011; 28(11):2377–87. [PubMed: 21473683]

48. Lee P, Lin R, Moon J, Lee LP. Microfluidic alignment of collagen fibers for in vitro cell culture. Biomed Microdevices. 2006; 8(1):35–41. [PubMed: 16491329]

49. Verdu E, Labrador RO, Rodriguez FJ, Ceballos D, Fores J, Navarro X. Alignment of collagen and laminin-containing gels improve nerve regeneration within silicone tubes. Restor Neurol Neurosci. 2002; 20(5):169–79. [PubMed: 12515893]

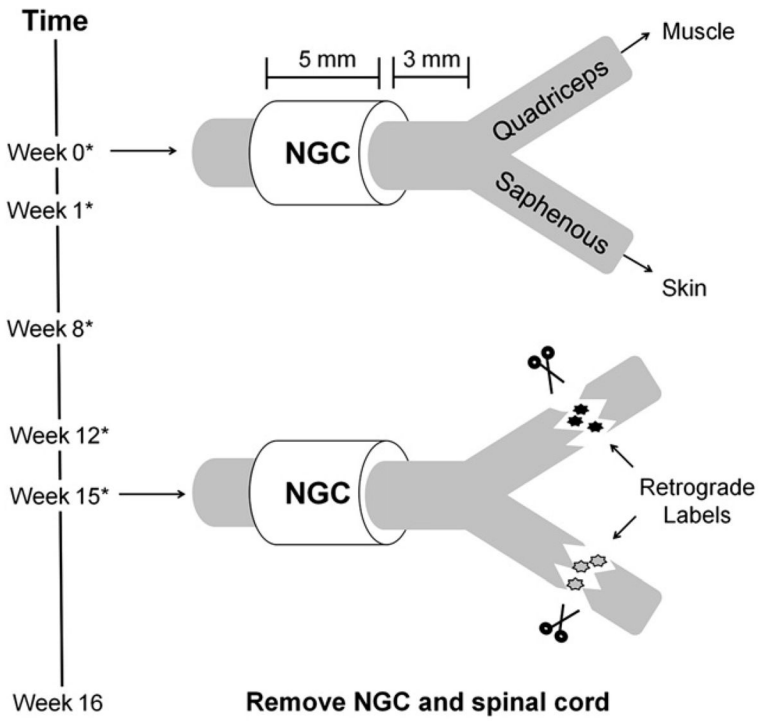

Fig. 1.

Schematic of femoral nerve injury model. The femoral nerve bifurcates into the quadriceps branch, which is innervated by motor and sensory axons, and the saphenous branch, which is innervated by only sensory axons. At week 0, the intact nerve was transected 3 mm proximal to the point of bifurcation and a prefilled nerve guidance conduit (NGC) was sutured in place with an imposed 5 mm gap. At 15 weeks post injury, retrograde labels were introduced into the branches 5 mm distal to the point of bifurcation to evaluate if regenerating motor axons selected the correct branch. One week later, the animal was sacrificed and the regenerated nerve and spinal cord were excised. An asterisk (*) signifies weeks in which animals were filmed to assess functional recovery.

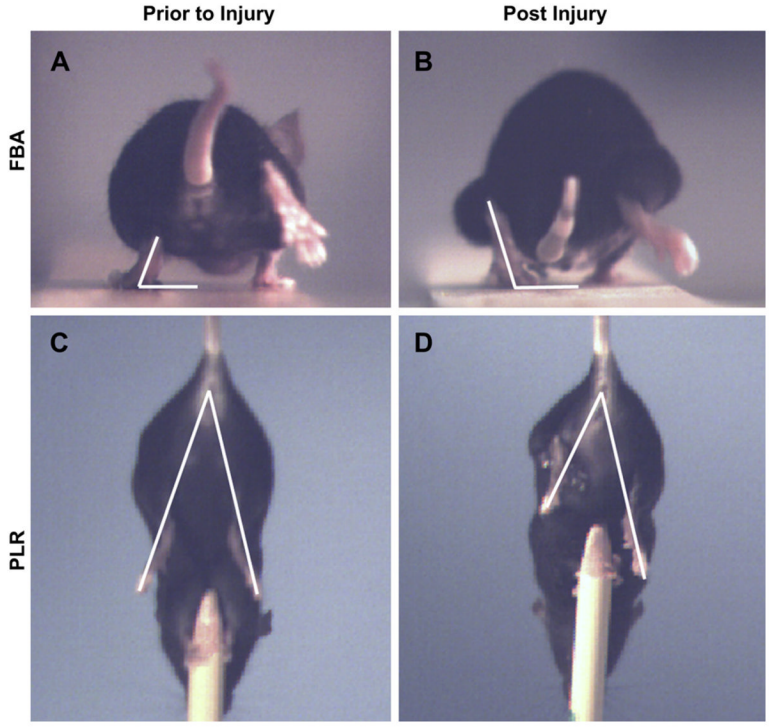

Fig. 2.

Single frame motion analysis. Representative single frames extracted from high-speed videos where individual frames were used to assess effective quadriceps function at specific points within each movement cycle. (A–B): The foot base angle (FBA) was measured at the point where the ipsilateral leg is at its highest point. (C–D) The protraction limb ratio (PLR) was measured when there is complete vertical extension towards the fixed object below. Measurements are taken prior to injury (A, C) and periodically during the first 15 weeks following injury (B, D).

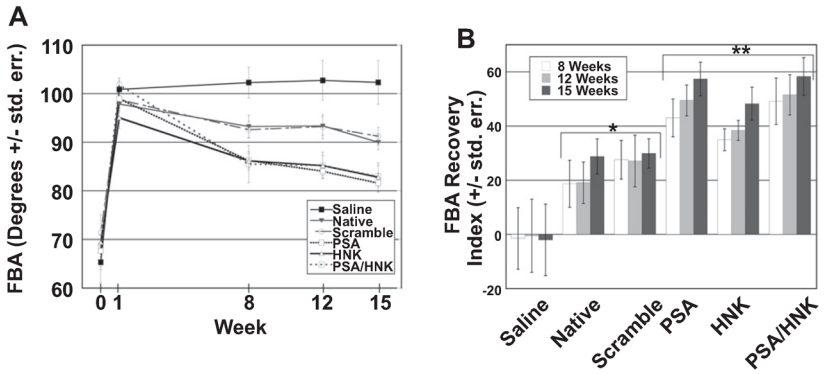

Fig. 3.

Functional evaluation of quadriceps reinnervation as assessed using foot base angle (FBA). (A) Evaluation of FBA measurements over time revealed significantly reduced angles at weeks 8, 12, and 15 between collagen and saline treated groups, and between glycomimetic peptide-coupled and non-glycomimetic peptide-coupled groups. No statistical differences were found among groups treated with glycomimetic peptide-coupled collagen or between and native collagen and scrambled peptide-coupled groups at any of these time points. (B) When FBA measurements were normalized to the extent of injury at week 1 using the recovery index, statistically significant differences are seen at weeks 8, 12, and 15 between collagen and saline treated groups. No statistical differences were found among glycomimetic treated groups or between native and scrambled peptide-coupled groups at any of these time point. An asterisk (*) signifies statistically significant differences verses saline when compared to its respective time point. A double asterisk (**) signifies statistically significant differences versus saline, native, and scrambled peptide-coupled collagen when compared to its respective time point. Means are reported +/− standard error. Differences were considered significant at $p < 0.05$ using one-way analysis of variance.

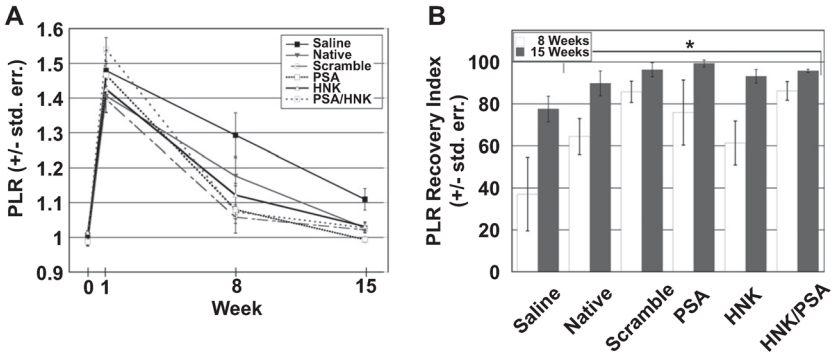

Fig. 4.

Functional evaluation of quadriceps branch reinnervation as assessed using protraction limb ratio (PLR). Evaluation of PLR measurements over time (A) and after normalizing to the extent of injury using the recovery index (B) revealed statistically significant differences at weeks 8 and 15 between collagen and saline treated groups as signified by an asterisk (*). However, no significant differences were found among collagen treated groups at either 8 or 15 weeks post injury. Means are reported +/− standard error. Differences were considered significant at $p < 0.05$ using one-way analysis of variance.

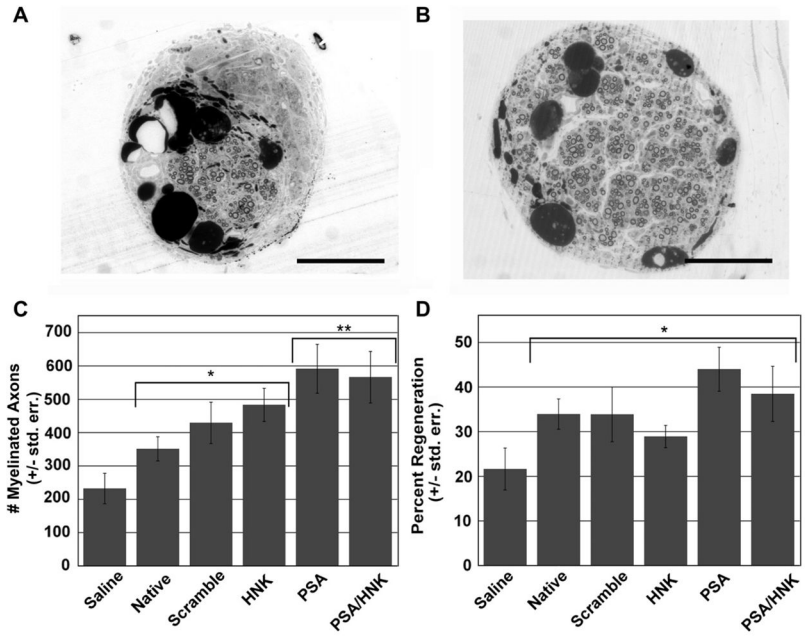

Fig. 5.

Histomorphometry of regenerated nerve. Representative images of osmium tetroxide stained saline (A) and glycomimetic peptide-coupled collagen (B) treated cross-sections from the middle of regenerated nerves at 16 weeks post-injury. (C) Evaluation of myelinated axon number revealed significantly more axons in collagen hydrogel verses saline treated groups, and between PSA containing hydrogels and non-PSA containing hydrogels. (D) Grafts with collagen hydrogels yielded a significantly greater percentage of nerve regeneration compared to saline treated animals. No statistical differences were noted between collagen treated groups. An asterisk (*) signifies statistically significant differences when compared to saline. A double asterisk (**) signifies statistically significant differences when compared to native, scrambled peptide-coupled, and HNK-coupled groups. Means are reported +/− standard error. Differences were considered significant at $p < 0.05$ using one-way analysis of variance. Scale bar represents 200 μm.

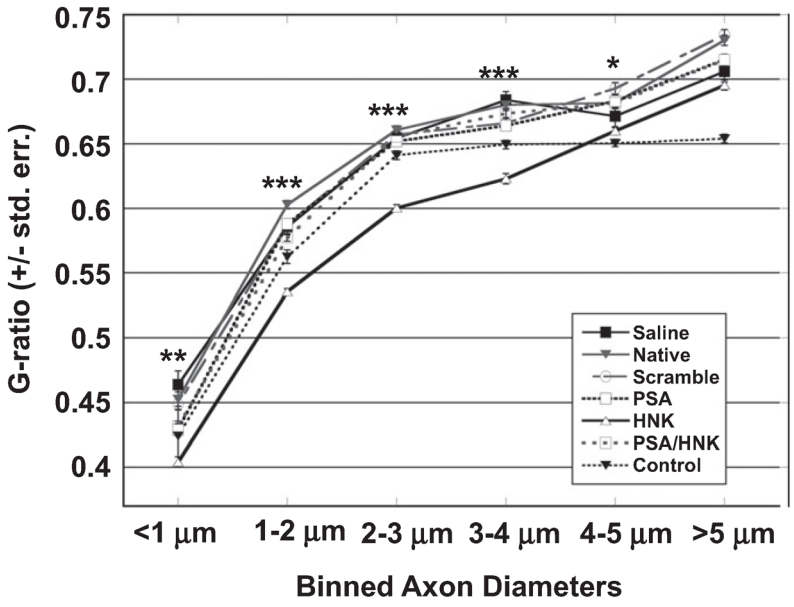

Fig. 6.

Effect of HNK-coupled hydrogels on g-ratio distribution in femoral nerve cross-sections. Measured g-ratios were binned with respect to axon size. Each bin was tested for statistical significance using a one-way ANOVA. Small caliber axons (<1 μm) treated with HNK-coupled hydrogels yield significantly lower g-ratios compared to all other groups (**). Axons between 1 and 4 μm in diameter yielded significantly lower g-ratios in HNK-coupled collagen treated nerves compared to both intact and regenerated nerves (***). Axons between 4 and 5 μm in diameter yielded significantly lower g-ratios than other collagen-treated groups, but not saline-treated or intact nerves (*). No significant differences were found with inclusion of HNK-coupled hydrogels for large caliber axons (>5 μm). Means are reported +/− standard error. Differences were considered significant at $p < 0.05$ using one-way analysis of variance.

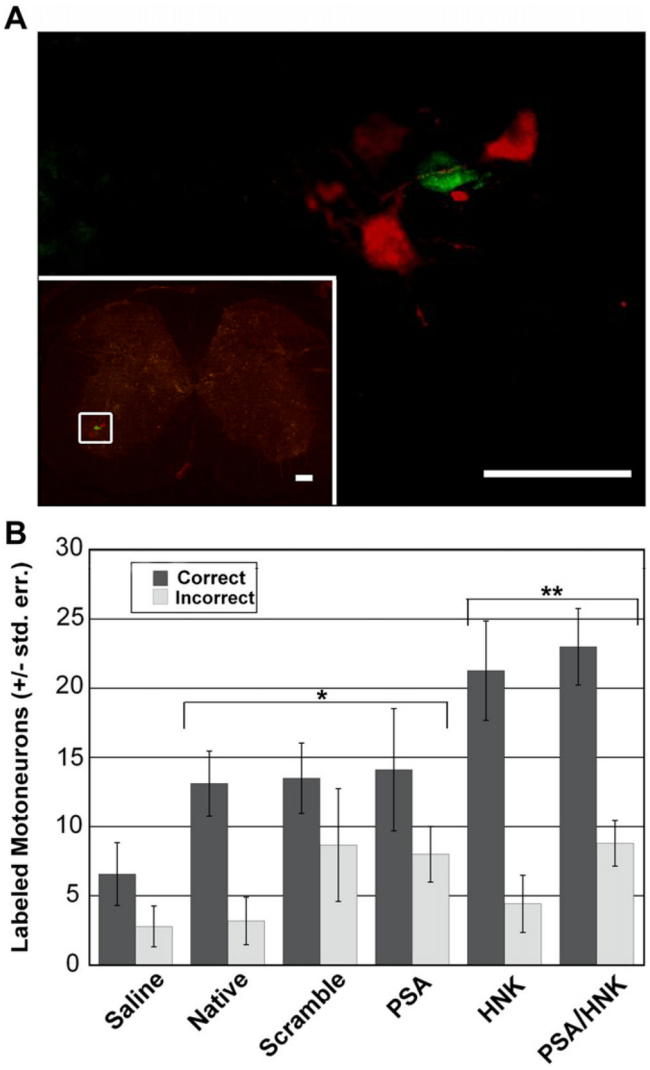

Fig. 7.

Analysis of retrogradely-labeled motoneurons. (A) Representative optical slice of correctly (red) and incorrectly (green) labeled motoneuronal cell bodies in cross-sections from spinal cords within the lumbar enlargement. Inset shows that fluorescently tagged retrograde labels were restricted to the motoneuron-rich ventral horn ipsilateral to the injured side. Longer exposure times were used to enhance autofluoresence in order to visualize the spinal cord structure in the inset. The higher magnification image shows distinguishable cell bodies used for motoneuron counts. Scale bars represent 100 μm. (B) Statistical analysis revealed significantly more correctly labeled motoneurons in all collagen-treated versus saline treated groups. Within hydrogel-treated conditions, groups containing coupled HNK-1 peptide resulted in significantly more correctly labeled motoneurons than groups without coupled HNK. No statistically significant differences were found between PSA and non-PSA containing collagen-treated animals, number of incorrectly labeled motoneurons, and total number of motoneurons. An asterisk (*) represents statistically significant differences compared to saline treated groups in number of correctly labeled motoneurons. A double asterisk (**) represents statistically significant differences of HNK- and PSA/HNK-coupled hydrogels compared to saline, native, scrambled peptide-coupled, and PSA-coupled in number of correctly projecting motoneurons. Means are reported +/− standard error.

Differences were considered significant at $p < 0.05$ using one-way analysis of variance. (For interpretation of the references to color in this figure legend, the reader is referred to the web version of this article.)

Table 1

Summary of functional and morphological results as assessed sixteen weeks post injury.

	Functional scores		Morphological scores			
	FBA	**PLR**	**Axon #**	**% Reg.**	**G-ratio**	**Motoneurons**
Saline	−	+	−	−	+	−
Native	+	++	+	+	+	+
Scrambled	+	++	+	+	+	+
PSA	++	++	++	++	+	+
HNK	++	++	+	+	++	++
PSA/HNK	++	++	++	++	+	++

A ‘−’ denotes no improvement from week one scores, a ‘+’ denotes moderate improvement, and ‘++’ denotes greatest improvement relative to other conditions.